A Robust Mixed-Conducting Multichannel Hollow Fiber Membrane Reactor

Jiawei Zhu, Shaobin Guo, Gongping Liu, Zhengkun Liu, Zhicheng Zhang, and Wanqin Jin
State Key Laboratory of Materials-Oriented Chemical Engineering, College of Chemistry and Chemical Engineering, Nanjing Tech University (former Nanjing University of Technology), 5 Xinmofan Road, Nanjing 210009, P.R. China

DOI 10.1002/aic.14835
Published online April 20, 2015 in Wiley Online Library (wileyonlinelibrary.com)

To accelerate the commercial application of mixed-conducting membrane reactor for catalytic reaction processes, a robust mixed-conducting multichannel hollow fiber (MCMHF) membrane reactor was constructed and characterized in this work. The MCMHF membrane based on reduction-tolerant and CO_2-stable $SrFe_{0.8}Nb_{0.2}O_{3-\delta}$ (SFN) oxide not only possesses a good mechanical strength but also has a high oxygen permeation flux under air/He gradient, which is about four times that of SFN disk membrane. When partial oxidation of methane (POM) was performed in the MCMHF membrane reactor, excellent reaction performance (oxygen flux of 19.2 mL min^{-1} cm^{-2}, hydrogen production rate of 54.7 mL min^{-1} cm^{-2}, methane conversion of 94.6% and the CO selectivity of 99%) was achieved at 1173 K. And also, the MCMHF membrane reactor for POM reaction was operated stably for 120 h without obvious degradation of reaction performance. *AIChE J*, 61: 2592–2599, 2015
Keywords: mixed-conducting membrane, multichannel hollow fiber membrane, membrane reactor, methane conversion

Introduction

Due to the potential impacts on energy and environment, mixed-conducting dense membranes have attracted considerable interests in many promising application areas, such as oxygen separation,[1–7] solid oxide fuel cells,[8] effective utilization of natural gas[9–14] or coke oven gas,[15,16] production of hydrogen,[17–20] as well as treatment of CO_2[21–23] and NO_x.[24,25] Among these applications, one of the most attractive applications of mixed-conducting membranes is to construct catalytic membrane reactor applied in the field of energy and environment. Mixed-conducting membrane reactors not only carry out separation and reaction in one unit but also potentially lead to achieve a green and sustainable chemistry with less energy consumption and pollution and improved performance in terms of separation, selectivity, and yield.[26,27] However, the commercialization of this concept has not been realized. For potential industrial or commercial applications, mixed-conducting membrane reactors should meet the following requirements: high permeation flux, adequate mechanical strength, excellent phase stability under reaction atmospheres, and attractive membrane configuration for industrial application.

Membrane configuration is as important as membrane materials in determining the performance of reaction in mixed-conducting membrane reactors. Currently, single-channel hollow fiber membranes successfully fabricated by phase inversion and sintering technique possess a thin wall and an asymmetric structure. This kind of membrane configuration presents prominent advantages over the conventional disk[6,28,29] or tubular configurations:[30–32] (1) much larger surface/volume ratios, (2) the thin separating dense layer results in high oxygen permeation flux, (3) the porous layers of the membrane provide much larger gas-membrane interfaces, resulting in a decrease of surface exchange resistances for gas transport.[2,7,33–37] Therefore, according to the above advantages, the configuration of hollow fiber is considered as the most promising one for the future industrial application in reaction process. More and more articles have reported the application of hollow fiber mixed-conducting membranes in reaction processes.[19,38–41] However, the single-channel hollow fiber membrane for reaction process may suffer from low mechanical strength because of thin membrane walls with a lot of finger or sponge-like pores. In our recent work,[42] a mixed-conducting multichannel hollow fiber (MCMHF) membrane was first proposed to overcome some drawbacks of conventional single-channel hollow fiber membranes for oxygen separation. Subsequently, from the viewpoint of making better use of the MCMHF membrane for oxygen separation, we systematically studied the effect of permeation modes on separation performance of the membrane.[43] So far, no research relates to application of the MCMHF membrane in reaction process. The membrane reactor performance in terms of mechanical strength, separation, reaction conversion, selectivity, and yield may be enhanced by such membrane configuration.

Therefore, the aim of this work is to construct and characterize a multichannel hollow fiber membrane reactor in catalytic reaction process. And the reaction of partial oxidation of methane (POM) ($CH_4 + \frac{1}{2}O_2 = CO + 2H_2$, $\Delta H^0_{298} = -36$ kJ mol^{-1})

Correspondence concerning this article should be addressed to W. Jin at wqjin@njtech.edu.cn.

will be performed in the MCMHF membrane reactor. The phase stability of the membrane material under reducing and CO_2 atmosphere, morphology, mechanical strength and the reaction performance of the MCMHF membrane reactor were investigated in detail.

Experimental

Synthesis of powder and preparation of the MCMHF membrane

The $SrFe_{0.8}Nb_{0.2}O_{3-\delta}$ (SFN) oxide with excellent stability and a high and steady oxygen flux[44] was selected to construct the MCMHF membrane reactor for POM reaction. SFN powder was synthesized by using solid-state reaction method. Stoichiometric amounts of $SrCO_3$ (99.9%), Fe_2O_3 (99.9%), and Nb_2O_5 (99.9%) were mixed and ball-milled in ethanol for 24 h and then dried. After calcination at 1563 K for 10 h in air, the SFN oxide was formed. And then the SFN powder was grinded and sieved via a sieve of 300 meshes for spinning the MCMHF membrane. The MCMHF membrane was fabricated using phase inversion/sintering technique. SFN powder, 1-methyl-2-pyrrolidinone (NMP), and polyethersulfone (PESf) in the mass ratio of 8:4:1 composed the spinning suspension. The membrane precursor was obtained by a tetra-bore spinneret reported in our previous work.[42] The internal and external coagulants were composed of deionized water and tape water, respectively. Subsequently, the SFN multichannel hollow fiber precursor was dried and then sintered at 1613 K in air for 10 h.

Characterizations

The crystal phase structures of the SFN powder and the hollow fiber membranes were observed by x-ray diffraction (XRD, Bruker, model D8 Advance) with Cu Kα radiation. The diffraction patterns from the samples were collected at ambient temperature by step scanning in the range of $20° \leq 2\ \theta \leq 80°$. Morphologies of the MCMHF membranes were detected by using a scanning electron microscope (SEM, Hitachi S-4800, Japan). The measurement of the mechanical strength of the MCMHF membrane was performed by using a tensile tester (Model CMT6203) with a load cell for 5 kN through a three-point bending test. The multichannel hollow fiber membrane samples were fixed in the sample holder with a length of 50 mm. The crosshead speed was fixed at 0.02 cm min^{-1}. The minimum load (F_m) needed to break the sample was recorded.

Membrane reactor setup

The measurement of oxygen permeation fluxes of the gas-tight and defect-free MCMHF membranes was performed by using a home-made apparatus.[43,45] A multichannel hollow fiber membrane sample with the length of about 20 mm was sealed by silver with the two dense alumina tubes. The lumen side of the membrane was exposed to pure helium and the shell side was fed by air. The temperature surrounding the membrane was monitored by a programmable temperature controller (Model AI-708PA, Xiamen Yudian automation technology Co.). The mass flow controllers (Model D07-19B, Beijing Jianzhong Machine Factory, China) controlled inlet gas flow rates. Both the shell and lumen sides of the MCMHF membrane were under the atmospheric pressure. The on-line gas chromatograph (GC, Shimadzu, model GC-8A, Japan) was used to analyze the composition of effluent streams from the sweep side. The effective membrane area is about 0.8 cm^2 in this measurement. The more details about obtaining the oxygen permeation flux of the MCMHF membrane can be seen in our previous work.[42]

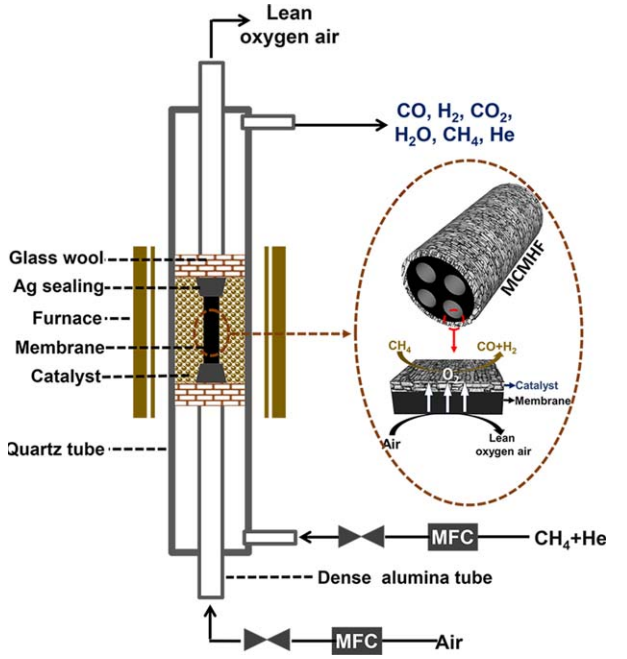

Figure 1. Illustration of the MCMHF membrane reactor module for POM reaction.

[Color figure can be viewed in the online issue, which is available at wileyonlinelibrary.com.]

The MCMHF membrane reactor for POM reaction experiment is shown in Figure 1. The effective length of the MCMHF membrane was 3.0 mm. one gram 40–60 mesh Ni/Al_2O_3 catalyst was packed on the shell side of the MCMHF membrane. POM reaction occurs at the shell side of the MCMHF membrane. More clearly, methane reacts with oxygen, which permeates through the membrane from the lumen side of the membrane, to produce hydrogen and CO over supported catalysts. The shell side of the membrane was exposed to the mixture of CH_4 and He, and air was fed to the lumen side of the membrane. In this work, both sides of the membrane reactor were maintained at atmospheric pressure. The composition of effluent streams was analyzed by two on-line GC (Shimadzu, model GC-8A, Japan) equipped with a 5Å molecule sieve column and a TDX-01 column, respectively. The 5Å molecule sieve column was used for the detection of H_2, O_2, N_2, CH_4, and CO, and the TDX-01 column was used for detecting H_2, CH_4, and CO_2. The oxygen permeation fluxes through the MCMHF membrane reactor were calculated from the effluent flow rate and the concentration of oxygen-containing compounds in the effluent. The oxygen permeation flux (J_{O_2}), hydrogen production rate (P_{H_2}), CH_4 conversion (X_{CH_4}), CO selectivity (S_{CO}) were calculated by the following equations

$$X_{CH_4} = \left(F_{CH_4,\,inlet} - F_{CH_4,\,outlet}\right)/F_{CH_4,\,inlet} \quad (1)$$

$$S_{CO} = F_{CO}/\left(F_{CH_4,\,inlet} - F_{CH_4,\,outlet}\right) \quad (2)$$

$$P_{H_2} = F_{H_2}/A \quad (3)$$

where F_i is the flow rate of species i. A is about 0.245 cm^2. The oxygen permeation flux through the multichannel hollow

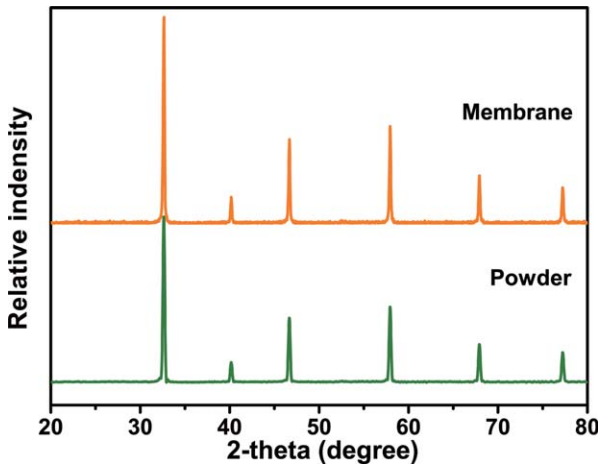

Figure 2. XRD patterns of SFN fresh powder and fresh membrane.

[Color figure can be viewed in the online issue, which is available at wileyonlinelibrary.com.]

fiber membrane reactor could be obtained by the mass balance on the basis of the components of CO, CO_2, O_2, and H_2O in the exit stream

$$J_{O_2} = (F_{CO} + 2F_{CO_2} + F_{H_2O} + 2F_{O_2}(\text{unreacted}))/2A \quad (4)$$

where F_{H_2O} can be calculated according to the hydrogen balance

$$F_{CH_4,\text{inlet}} = F_{CH_4,\text{outlet}} + \frac{1}{2}F_{H_2} + \frac{1}{2}F_{H_2O} \quad (5)$$

Substitution Eq. 4 to Eq. 3 yields

$$J_{O_2} = (F_{CO} + 2F_{CO_2} + 2F_{CH_4,\text{inlet}} - 2F_{CH_4,\text{outlet}} - F_{H_2} + 2F_{O_2}(\text{unreacted}))/2A \quad (6)$$

Results and Discussion

Crystalline structure and chemical stability of membrane material

The XRD patterns of the as-synthesized SFN powder and the as-prepared MCMHF membrane sintered at 1613 K for 10 h are shown in Figure 2. XRD analysis showed that both the samples of SFN powder and SFN membrane have well-formed perovskite crystalline structure.

Because POM reaction environment contained reducing gases (H_2) and a small amount of CO_2, the membrane material applied in POM reaction must possess excellent chemical stability at elevated temperatures in reducing and CO_2-contianed atmosphere. To evaluate the chemical stability, we exposed SFN powder samples to 5 vol % H_2/Ar and pure CO_2 at 1173 K for 20 h, respectively. As shown in Figure 3, SFN oxide still maintained full perovskite structure and no obvious new phases can be found after being treated in both reducing and CO_2 atmospheres at 1173 K for 20 h. Additionally, it should be noticed that the characteristic peaks of the SFN powder shifted slightly to a lower angle after treatment in reducing atmosphere. The result should be correlated with the increase in the cell parameter because of the loss of lattice oxygen in the perovskite structure during the treatment under reducing atmosphere.[13] These results demonstrated that SFN oxide exhibited a good chemical stability at high temperature and under both reducing and CO_2 atmospheres.

Morphologies of the sintered MCMHF membrane

Figure 4 shows the morphologies of the sintered MCMHF membrane. Figure 4a visually shows that the inner and outer diameters of the sintered membrane were about 0.78 mm and 2.6 mm, respectively. Figure 4b displays the wall structures of the membrane. Finger-like pores appeared at the center wall of the membrane, and sponge-like structures were near the outer and inner wall of the membrane. The formation of the complex structures in the MCMHF membrane can be attributed to the complicated interactions between the spinning suspension and nonsolvent. More details about the formation process of the complex structure can be obtained in the literatures.[7,40,42] The thickness of the membrane dense layer could be simply considered as about 80 μm clearly shown in Figure 4b. The very dense structures of the membrane surfaces which were formed during controllable sintering process are clearly shown in Figures 4c,d.

Breaking load of the sintered MCMHF membrane

The breaking load of the mixed-conducting hollow fiber membrane reactors is of significance for their practical application. By three-point bending test, we can found that the as-prepared MCMHF membrane can withstand a breaking load of about 20 N, which was about 20 times that of conventional single-channel hollow fiber membranes.[46–48] The special cross-shaped structure of the MCMHF membrane shown in Figure 4a could play a supporting role in bearing the force applied on the membrane and then provide an excellent breaking load value for the membrane. This excellent mechanical strength can make the MCMHF membrane reactor be a potential candidate for industrial application.

Membrane reactor performance

In general, the oxygen permeation flux of MCMHF membrane is a significant factor in the production rate of syngas because the consumption of 1 mol O_2 will produce 4 mol H_2 and 2 mol CO in the POM reaction. Figure 5 shows the

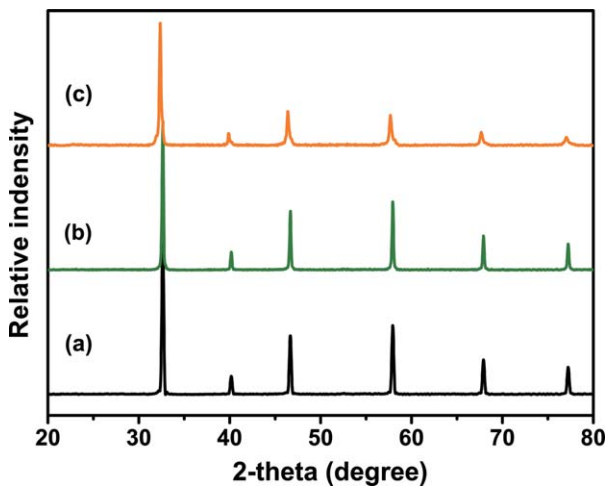

Figure 3. XRD patterns of SFN samples.

(a) fresh powder; (b) powder annealed in pure CO_2 at 1173 K for 20 h; and (c) powder annealed in in 5vol % H_2/Ar atmosphere at 1173 K for 20 h. [Color figure can be viewed in the online issue, which is available at wileyonlinelibrary.com.]

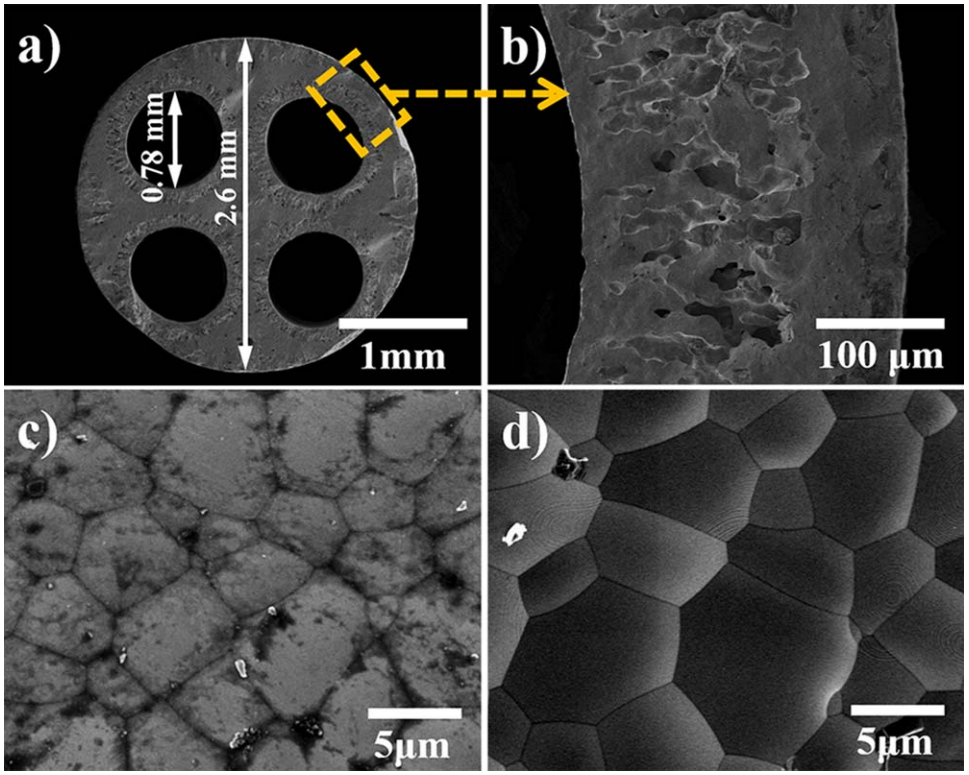

Figure 4. SEM images of as-prepared MCMHF membrane.

(a) cross section of the fresh membrane; (b) the wall of the fresh membrane; (c) outer surface of the fresh membrane; and (d) inner surface of the fresh membrane. [Color figure can be viewed in the online issue, which is available at wileyonlinelibrary.com.]

temperature dependence of the oxygen permeation flux with He as sweep gas in the temperature range of 1073–1173 K. As known to all, temperature has a significant influence on oxygen permeation flux. The oxygen permeation flux increases with increasing temperature because of the reduction of the oxygen bulk diffusion resistance and the oxygen surface reaction resistance. The oxygen permeation flux increased from 0.50 to 1.21 mL min^{-1} cm^{-2} by increasing the temperatures from 1073 to 1173 K. Nevertheless, for a disk SFN membrane, Yi et al reported that oxygen permeation fluxes of the membrane was about 0.31 mL min^{-1} cm^{-2} at 1173 K.[44] Thus, the oxygen permeation flux of our MCMHF membrane was about four times that of conventional disk membrane with membrane thickness of 1 mm. The possible reason could be that the dense layer of the MCMHF membrane is much thinner than that of the symmetric disk membrane. Therefore, MCMHF membrane can obtain high oxygen flux and will be a potential candidate to construct membrane reactor applied in the field of energy and environmental.

The operating conditions such as reaction temperature, methane flow rate, air flow rate, helium flow rate, and methane concentration will greatly affect the reaction performance in terms of oxygen permeation flux, hydrogen production rate, methane conversion, and CO selectivity. Thus, we investigate the influence of above operating conditions on the performance of the SFN MCMHF membrane reactor in detail as follows.

The POM reaction performance of the MCMHF membrane reactor in the temperature range of 1023–1173 K was investigated. Figure 6 shows the temperature dependence of the performance of SFN membrane reactor. Each temperature point was held about 0.5 h and all the corresponding data points were recorded for at least three times for ensuring the accuracy of the experiment results. As we all known, temperature could influence the performance of membrane reaction significantly. Oxygen permeation flux, hydrogen production rate, and methane conversion increase rapidly with increasing the temperature. The increase of oxygen permeation flux was mainly attributed to the increase of oxygen bulk diffusion rate and surface exchange kinetics by increasing the reaction temperature. For the excess feed of the methane, the methane conversion was mainly controlled by

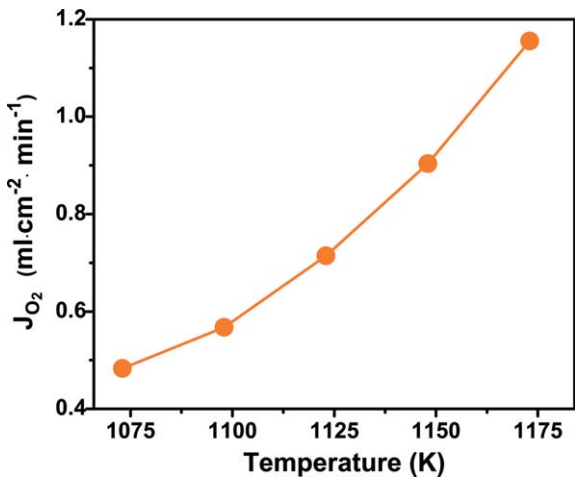

Figure 5. Oxygen permeation fluxes of MCMHF membrane as a function of temperature (F_{Air} = 120 mL min^{-1}, F_{He} = 80 mL min^{-1}).

[Color figure can be viewed in the online issue, which is available at wileyonlinelibrary.com.]

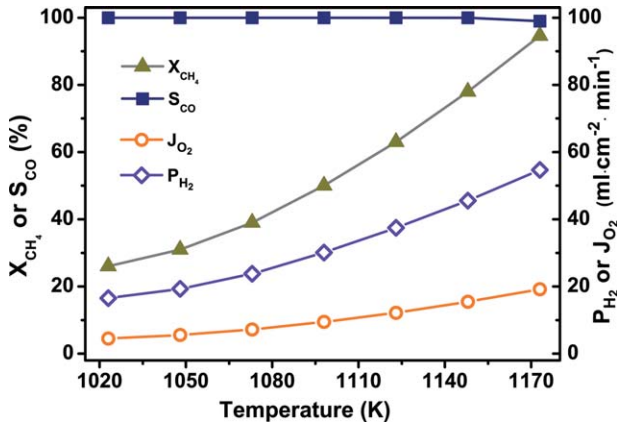

Figure 6. CO selectivity, CH_4 conversion, H_2 production rate, and oxygen permeation flux as a function of temperature ($F_{CH_4} = 8$ mL min^{-1}, $F_{He} = 40$ mL min^{-1}, $F_{air} = 80$ mL min^{-1}).

[Color figure can be viewed in the online issue, which is available at wileyonlinelibrary.com.]

the oxygen permeation flux. Therefore, the increase in methane conversion was caused by the increased oxygen permeation flux.[13] At 1173 K, the oxygen permeation flux is about 19.2 mL min^{-1} cm^{-2}, which is a remarkable value because the oxygen permeation flux exceeding 15 mL min^{-1} cm^{-2} is rarely obtained. And the methane conversion is 94.6%, the CO selectivity is about 99% and the hydrogen production rate is about 54.7 mL min^{-1} cm^{-2}. By comparison, the oxygen flux of the MCMHF membrane reactor is about 16 and 62 times that of the MCMHF membrane and SFN disk membrane with thickness of 1mm, respectively, under the air/He gradient. The reasons for this are as follows: (1) under the air/CH_4 gradient, the oxygen partial pressure at the permeated side is very lower than that under the air/He gradient and then the lower oxygen partial pressure improves the driving force for oxygen transport according to Wagner's equation,[27] (2) the dense layer of the MCMHF membrane is obviously thinner than that of SFN disk membrane. The CO selectivity keeps the constant of 100% when the temperature is below 1123 K and it decreases when the temperature is higher than 1123 K. The reason for this experiment phenomena is that the ratio of methane and oxygen deceased at high temperatures due to the oxygen flux increased with increasing temperature, which led to the excessive oxidation of CO. Similar explanations were reported by many researchers in the literatures.[17,49]

The effects of methane flow rate on CO selectivity, CH_4 conversion, hydrogen production rate, and oxygen permeation flux at 1173 K are shown in Figure 7. In this experiment, air of 80 mL min^{-1} was fed into the lumen side of the membrane reactor and the flow rate of helium was fixed at about 40 mL min^{-1} while the methane flow rate was increased from 4 to 16 mL min^{-1}.The methane conversion decreased and CO selectivity increased with increasing the methane flow rate. Oxygen permeation flux and hydrogen production rate increased rapidly with increasing the methane flow rate from 4 to12 mL min^{-1}, but when the methane flow rate further increased to 16 mL min^{-1}, the oxygen permeation flux and hydrogen production rate increased very slowly. These results can be explained as follows. According to the literatures,[22,50] the methane conversion mechanism in the MCMHF membrane reactor packed with Ni-based catalyst is the combustion reform reaction mechanism. When the methane flow rate is lower than 12 mL min^{-1}, the permeated oxygen is first reacted with part of fed methane to form CO_2 and H_2O on the surface of the membrane, and then the residual methane reacts with CO_2 and H_2O to produce CO and hydrogen. The oxygen permeation flux increased due to the decrease in oxygen partial pressure near the membrane surface. When the methane flow rate is higher than 12 mL min^{-1}, the increased methane mainly reacted with CO_2 and H_2O to form syngas rather than directly reacted with oxygen. Therefore, the oxygen partial pressure near the membrane surface would slightly decrease, which results in the slight increase of oxygen permeation flux. As presented in Eq. 1, the methane conversion can be expressed as the ratio of the reacted methane to the feed methane. Although the reacted methane slightly increases with increasing the oxygen permeation flux, the feed methane increases rapidly with increasing methane flow rate. Therefore, the methane conversion decreased drastically with increasing methane flow rate and the ratio of methane and oxygen increased leading to the increase of CO selectivity.

Figure 8 presents the influence of the feed methane concentrations on the MCMHF membrane reactor performance at the temperature of 1173 K. Similar to the investigation of the effect of methane flow rate, air flow rate is kept at 80 mL min^{-1}. The total feed flow rate of the mixture of methane and helium is 60 mL min^{-1}, and by adjusting the ratio of methane and helium, the different methane concentrations are obtained. The methane conversion decreased and CO selectivity increased with increasing the methane concentrations. Oxygen permeation flux and hydrogen production rate increased rapidly with increasing the methane concentrations from 5 to 13.3%, but when the methane concentrations further increased to 25%, the oxygen permeation flux and hydrogen production rate increased very slowly. All of these results are similar to those shown in Figure 7. And the reason for these results is also the same as that for explaining the results in Figure 7. When the methane concentration is 13.3%, the methane conversion is about 93% and the CO selectivity is about 99.8%, presenting that the

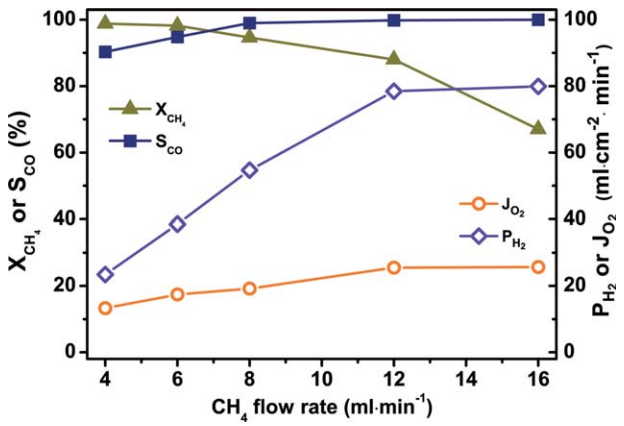

Figure 7. CO selectivity, CH_4 conversion, H_2 production rate, and oxygen permeation flux as a function of methane flow rate ($F_{He} = 40$ mL min^{-1}, $F_{air} = 80$ mL min^{-1}, Temperature = 1173 K).

[Color figure can be viewed in the online issue, which is available at wileyonlinelibrary.com.]

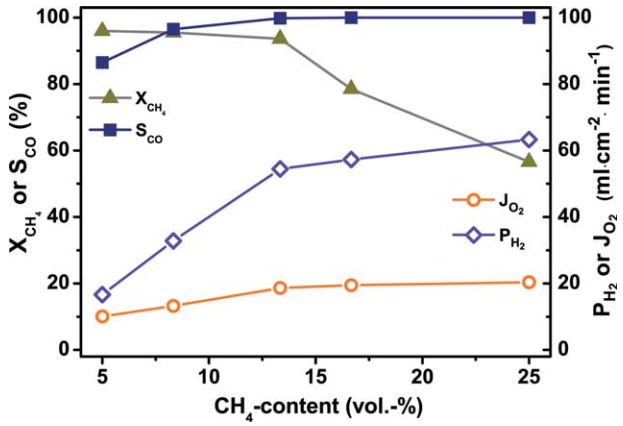

Figure 8. CO selectivity, CH_4 conversion, H_2 production rate and oxygen permeation flux as a function of methane concentration (F_{He}+ F_{CH_4} = 60 mL min^{-1}, F_{air} = 80 mL min^{-1}, Temperature = 1173 K).

[Color figure can be viewed in the online issue, which is available at wileyonlinelibrary.com.]

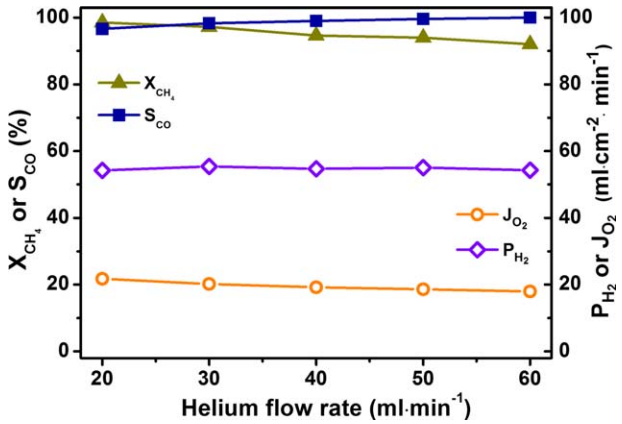

Figure 10. Helium flow rate dependence of POM reaction performance in MCMHF membrane (F_{CH_4} = 8 mL min^{-1}, F_{Air} = 80 mL min^{-1}, Temperature = 1173 K).

[Color figure can be viewed in the online issue, which is available at wileyonlinelibrary.com.]

membrane reactor has an excellent reaction performance. Similar results were reported by other researchers.[50]

The effect of feed air flow rate on reactor performance at 1173 K was presented in Figure 9. From Figure 9, we can see that the effects of air flow rate on oxygen permeation flux, hydrogen production rate, methane conversion, and CO selectivity of the MCMHF membrane reactor were insignificant when air flow rate is higher than 40 mL min^{-1}. These experimental results indicated that the flow rate of feed air has no influence on the oxygen permeation when the air flow rate is higher than 40 mL min^{-1}. Therefore, there is no need to further increase the air flow rate when the feed air is sufficient for supplying unchanged oxygen permeation flux. Similar results like these were reported in the literatures.[13,51]

Figure 10 shows the effect of helium flow rate on reaction performance at 1173 K. In this experiment, the methane partial pressure was changed by fixing methane flow rate at 8 mL min^{-1} and varying the helium flow rate from 20 to 60 mL min^{-1}. As shown in Figure 10, the methane conversion decreased from 98.5 to 92% with increasing the flow rate of helium from 20 to 60 mL min^{-1}. The reason for this result is that the increase of helium flow rate would result in the reduction of methane partial pressure in shell side of the membrane reactor. According to the literature,[52] the decreased methane partial pressure decreased the oxygen permeation flux, and then the methane conversion.

For practical applications, the MCMHF membrane reactor must exhibit long-term stability at elevated temperatures under reaction atmospheres. The stability of the MCMHF membrane reactor at 1173 K over more than 120 h are shown in Figure 11. During this period, the methane conversion, CO selectivity, oxygen permeation flux, and hydrogen production rate remained at about 94%, 99%, 19 mL min^{-1} cm^{-2}, and 54 mL min^{-1} cm^{-2}, respectively. These results indicated that the SFN MCMHF membrane reactor exhibits excellent performance and good stability for methane conversion. The experiment was voluntarily stopped when the reaction had continued for about 123 h. The methane side surface phase composition of the used MCMHF membrane

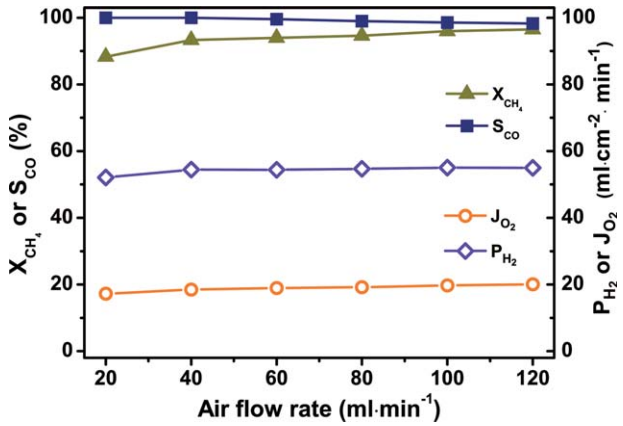

Figure 9. Air flow rate dependence of POM reaction performance in MCMHF membrane (F_{CH_4} = 8 mL min^{-1}, F_{He} = 40 mL min^{-1}, Temperature = 1173 K).

[Color figure can be viewed in the online issue, which is available at wileyonlinelibrary.com.]

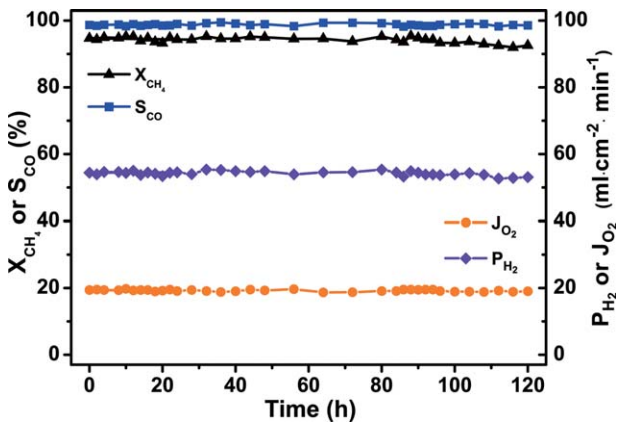

Figure 11. Time dependence of POM reaction performance in MCMHF membrane (F_{CH_4} = 8 mL min^{-1}, F_{He} = 40 mL min^{-1}, F_{Air} = 80 mL min^{-1}, Temperature = 1173 K).

[Color figure can be viewed in the online issue, which is available at wileyonlinelibrary.com.]

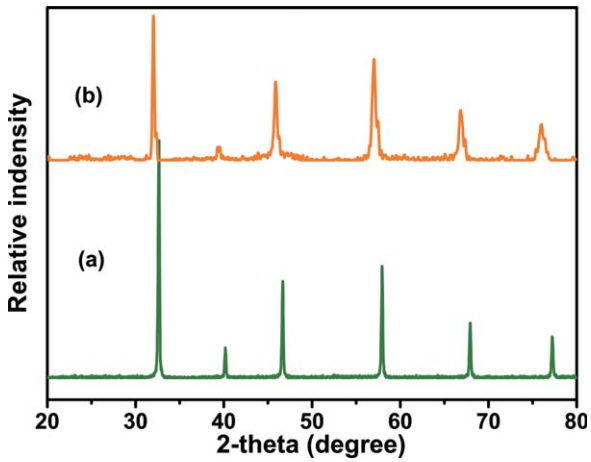

Figure 12. XRD patterns of SFN samples.

(a) fresh membrane and (b) outer surface of MCMHF membrane after 120 h POM reaction. [Color figure can be viewed in the online issue, which is available at wileyonlinelibrary.com.]

was detected by XRD shown in Figure 12. Very little impurity phase can be observed and the perovskite main phase still exists after 120 h POM reaction. However, the perovskite main phase exists after 120 h POM operation.

The excellent performance of the SFN MCMHF membrane reactor may be attributed to three aspects. First, as discussed above, the good chemical stability of the SFN oxide under both reducing and CO_2 atmospheres is very important to ensure the membrane stability under POM reaction atmosphere. Second, the MCMHF with superb mechanical strength can guarantee the preforming of the reaction process. Third, most importantly, the MCMHF membrane with very thin dense layer can obtain higher the oxygen permeation flux and then convert more methane into products compared to conventional disk or tubular membrane. All these indicate that multichannel hollow fiber is a potential membrane reactor configuration with good performance in membrane reaction.

Conclusions

We constructed and characterized the robust multichannel hollow fiber membrane reactor in POM reaction process in this work. The mechanical strength of the MCMHF membrane was very much higher than that of conventional single-channel hollow fiber membranes, which was very helpful to overcome some drawbacks of single-channel hollow fiber membranes and guarantee the preforming of the reaction process. POM was performed in the MCMHF membrane reactor in the presence of Ni-based catalyst. The oxygen permeation flux of the MCMHF membrane reactor was largely improved by the very thin dense layer of the membrane. In the reactor under the POM reaction condition, the maximum oxygen permeation flux reached 19.2 mL min^{-1} cm^{-2}, which is a very high value and is about 16 and 62 times that of SFN MCMHF membrane and SFN disk membrane obtained under air/He gradient, respectively. At the same time, 94.6% methane conversion, 99% CO selectivity, and a hydrogen production rate of 54.7 mL min^{-1} cm^{-2} have been achieved at 1173 K. And also, the SFN MCMHF membrane reactor was operated stably for 120 h without obvious degradation of reaction performance. Our work demonstrates that the membrane configuration of multichannel hollow fiber with excellent performance will be a potential candidate to construct catalytic membrane reactor applied in the field of energy and environmental.

Acknowledgments

This work was supported by the Innovative Research Team Program by the Ministry of Education of China (No. IRT13070) and the Project of Priority Academic Program Development of Jiangsu Higher Education Institutions (PAPD).

Literature Cited

1. Lin YS, Wang WJ, Han JH. Oxygen permeation through thin mixed-conducting solid oxide membranes. *AIChE J*. 1994;40:786–798.
2. Tablet C, Grubert G, Wang HH, et al. Oxygen permeation study of perovskite hollow fiber membranes. *Catal Today*. 2005;104:126–130.
3. Kim J, Lin YS. Synthesis and oxygen permeation properties of ceramic-metal dual-phase membranes. *J Member Sci*. 2000;167:123–133.
4. Jin WQ, Li SG, Huang P, Xu NP, Shi J. Preparation of an asymmetric perovskite-type membrane and its oxygen permeability. *J Member Sci*. 2001;185:237–243.
5. Li SG, Jin WQ, Huang P, Xu NP, Shi J, Lin YS. Tubular lanthanum cobaltite perovskite type membrane for oxygen permeation. *J Member Sci*. 2000;166:51–61.
6. Li SG, Jin WQ, Huang P, et al. Perovskite-related ZrO_2-doped $SrCo_{0.4}Fe_{0.6}O_{3\text{-delta}}$ membrane for oxygen permeation. *AIChE J*. 1999;45:276–284.
7. Liu S, Tan X, Shao Z, da Costa JCD. $Ba_{0.5}Sr_{0.5}Co_{0.8}Fe_{0.2}O_{3\text{-delta}}$ ceramic hollow-fiber membranes for oxygen permeation. *AIChE J*. 2006;52:3452–3461.
8. Shao ZP, Haile SM. A high-performance cathode for the next generation of solid-oxide fuel cells. *Nature*. 2004;431:170–173.
9. Cao Z, Jiang H, Luo H, et al. Natural gas to fuels and chemicals: improved methane aromatization in an oxygen-permeable membrane reactor. *Angew Chem Int Edit*. 2013;52:13794–13797.
10. Kniep J, Lin YS. Partial oxidation of methane and oxygen permeation in $SrCoFeO_x$ membrane reactor with different catalysts. *Ind Eng Chem Res*. 2011;50:7941–7948.
11. Shao ZP, Dong H, Xiong GX, Gong Y, Yang WS. Performance of a mixed-conducting ceramic membrane reactor with high oxygen permeability for methane conversion. *J Member Sci*. 2001;183:181–192.
12. Zhu X, Li Q, He Y, Cong Y, Yang W. Oxygen permeation and partial oxidation of methane in dual-phase membrane reactors. *J Member Sci*. 2010;360:454–460.
13. Jiang W, Zhang G, Liu Z, Zhang K, Jin W. A novel porous-dense dual-layer composite membrane reactor with long-term stability. *AIChE J*. 2013;59:4355–4363.
14. Dong X, Zhang C, Chang X, Jin W, Xu N. A self-catalytic membrane reactor based on a supported mixed-conducting membrane. *AIChE J*. 2008;54:1678–1680.
15. Cheng H, Zhang Y, Lu X, Ding W, Li Q. Hydrogen production from simulated hot coke oven gas by using oxygen-permeable ceramics. *Energ Fuel*. 2009;23:414–421.
16. Cheng H, Lu X, Hu D, Zhang Y, Ding W, Zhao H. Hydrogen production by catalytic partial oxidation of coke oven gas in $BaCo_{0.7}Fe_{0.2}Nb_{0.1}O_{3\text{-delta}}$ membranes with surface modification. *Int J Hydrogen Energy*. 2011;36:528–538.
17. Dong X, Liu Z, Jin W, Xu N. A self-catalytic mixed-conducting membrane reactor for effective production of hydrogen from methane. *J Power Sources*. 2008;185:1340–1347.
18. Zhu N, Dong X, Liu Z, Zhang G, Jin W, Xu N. Toward highly-effective and sustainable hydrogen production: bio-ethanol oxidative steam reforming coupled with water splitting in a thin tubular membrane reactor. *Chem Commun*. 2012;48:7137–7139.
19. Jiang H, Liang F, Czuprat O, et al. Hydrogen production by water dissociation in surface-modified $BaCo_xFe_yZr_{1\text{-}x\text{-}y}O_{3\text{-delta}}$ hollow-fiber membrane reactor with improved oxygen permeation. *Chem Eur J*. 2010;16:7898–7903.
20. Jiang H, Wang H, Werth S, Schiestel T, Caro J. Simultaneous production of hydrogen and synthesis gas by combining water splitting with partial oxidation of methane in a hollow-fiber membrane reactor. *Angew Chem Int Edit*. 2008;47:9341–9344.

21. Jin W, Zhang C, Chang X, Fan Y, Xing W, Xu N. Efficient catalytic decomposition of CO_2 to CO and O-2 over Pd/mixed-conducting oxide catalyst in an oxygen-permeable membrane reactor. *Environ Sci Technol*. 2008;42:3064–3068.
22. Zhang C, Jin W, Yang C, Xu N. Decomposition of CO_2 coupled with POM in a thin tubular oxygen-permeable membrane reactor. *Catal Today*. 2009;148:298–302.
23. Zhang K, Zhang G, Liu Z, Zhu J, Zhu N, Jin W. Enhanced stability of membrane reactor for thermal decomposition of CO_2 via porous-dense-porous triple-layer composite membrane. *J Member Sci*. 2014; 471:9–15.
24. Jiang H, Wang H, Liang F, Werth S, Schiestel T, Caro J. Direct decomposition of nitrous oxide to nitrogen by in situ oxygen removal with a perovskite membrane. *Angew Chem Int Edit*. 2009; 48:2983–2986.
25. Jiang H, Xing L, Czuprat O, et al. Highly effective NO decomposition by in situ removal of inhibitor oxygen using an oxygen transporting membrane. Chem Commun. 2009:6738–6740.
26. Dong X, Jin W, Xu N, Li K. Dense ceramic catalytic membranes and membrane reactors for energy and environmental applications. *Chem Commun*. 2011;47:10886–10902.
27. Wei Y, Yang W, Caro J, Wang H. Dense ceramic oxygen permeable membranes and catalytic membrane reactors. *Chem Eng J*. 2013; 220:185–203.
28. Zeng Y, Lin YS, Swartz SL. Perovskite-type ceramic membrane: synthesis, oxygen permeation and membrane reactor performance for oxidative coupling of methane. *J Member Sci*. 1998;150:87–98.
29. Dyer PN, Richards RE, Russek SL, Taylor DM. Ion transport membrane technology for oxygen separation and syngas production. *Solid State Ionics*. 2000;134:21–33.
30. Jin WQ, Li SG, Huang P, Xu NP, Shi J, Lin YS. Tubular lanthanum cobaltite perovskite-type membrane reactors for partial oxidation of methane to syngas. *J Member Sci*. 2000;166:13–22.
31. Wang HH, Cong Y, Yang WS. Oxygen permeation study in a tubular $Ba_{0.5}Sr_{0.5}Co_{0.8}Fe_{0.2}O_{3\text{-delta}}$ oxygen permeable membrane. *J Member Sci*. 2002;210:259–271.
32. Wang HH, Wang R, Liang DT, Yang WS. Experimental and modeling studies on $Ba_{0.5}Sr_{0.5}Co_{0.8}Fe_{0.2}O_{3\text{-delta}}$ (BSCF) tubular membranes for air separation. *J Member Sci*. 2004;243:405–415.
33. Czuprat O, Arnold M, Schirrmeister S, Schiestel T, Caro J. Influence of CO_2 on the oxygen permeation performance of perovskite-type $BaCo_xFe_yZr_zO_{3\text{-delta}}$ hollow fiber membranes. *J Member Sci*. 2010; 364:132–137.
34. Tan X, Liu N, Meng B, Sunarso J, Zhang K, Liu S. Oxygen permeation behavior of $La_{0.6}Sr_{0.4}Co_{0.2}Fe_{0.8}O_3$ hollow fibre membranes with highly concentrated CO_2 exposure. *J Member Sci*. 2012;389:216–222.
35. Wei Y, Liu H, Xue J, Li Z, Wang H. Preparation and oxygen permeation of U-shaped perovskite hollow-fiber membranes. *AIChE J*. 2011;57:975–984.
36. Sunarso J, Liu S, Lin YS, da Costa JCD. High performance BaBiScCo hollow fibre membranes for oxygen transport. *Energy Environ Sci*. 2011;4:2516–2519.
37. Tan X, Wang Z, Li K. Effects of sintering on the properties of $La_{0.6}Sr_{0.4}Co_{0.2}Fe_{0.8}O_{3\text{-delta}}$ Perovskite hollow fiber membranes. *Ind Eng Chem Res*. 2010;49:2895–2901.
38. Kathiraser Y, Kawi S. $La_{0.6}Sr_{0.4}Co_{0.8}Ga_{0.2}O_{3\text{-delta}}$ (LSCG) hollow fiber membrane reactor: partial oxidation of methane at medium temperature. *AIChE J*. 2013;59:3874–3885.
39. Wu Z, Wang B, Li K. Functional LSM-ScSZ/NiO-ScSZ dual-layer hollow fibres for partial oxidation of methane. *Int J Hydrogen Energy*. 2011;36:5334–5341.
40. Othman NH, Wu Z, Li K. A micro-structured $La_{0.6}Sr_{0.4}Co_{0.2}Fe_{0.8}O_{3\text{-delta}}$ hollow fibre membrane reactor for oxidative coupling of methane. *J Member Sci*. 2014;468:31–41.
41. Wu Z, Wang B, Li K. A novel dual-layer ceramic hollow fibre membrane reactor for methane conversion. *J Member Sci*. 2010;352: 63–70.
42. Zhu J, Dong Z, Liu Z, Zhang K, Zhang G, Jin W. Multichannel mixed-conducting hollow fiber membranes for oxygen separation. *AIChE J*. 2014;60:1969–1976.
43. Zhu J, Liu Z, Guo S, Jin W. Influence of permeation modes on oxygen permeability of the multichannel mixed-conducting hollow fibre membrane. *Chem Eng Sci*. 2015;122:614–621.
44. Yi J, Schroeder M, Martin M. CO2-Tolerant and cobalt-free SrFe0.8Nb0.2O3-delta Perovskite membrane for oxygen separation. *Chem Mater*. 2013;25:815–817.
45. Liu Z, Zhang G, Dong X, Jiang W, Jin W, Xu N. Fabrication of asymmetric tubular mixed-conducting dense membranes by a combined spin-spraying and co-sintering process. *J Member Sci*. 2012; 415:313–319.
46. Zydorczak B, Wu Z, Li K. Fabrication of ultrathin $La_{0.6}Sr_{0.4}Co_{0.2}Fe_{0.8}O_{3\text{-delta}}$ hollow fibre membranes for oxygen permeation. *Chem Eng Sci*. 2009;64:4383–4388.
47. Schiestel T, Kilgus M, Peter S, Caspary KJ, Wang H, Caro J. Hollow fibre perovskite membranes for oxygen separation. *J Member Sci*. 2005;258:1–4.
48. Leo A, Smart S, Liu S, da Costa JCD. High performance perovskite hollow fibres for oxygen separation. *J Member Sci*. 2011;368:64–68.
49. Bayraktar D, Clemens F, Diethelm S, Graule T, Van herle J, Holtappels P. Production and properties of substituted $LaFeO_3$-perovskite tubular membranes for partial oxidation of methane to syngas. *J Eur Ceram Soc*. 2007;27:2455–2461.
50. Zhang C, Chang X, Dong X, Jin W, Xu N. The oxidative stream reforming of methane to syngas in a thin tubular mixed-conducting membrane reactor. *J Member Sci*. 2008;320:401–406.
51. Li Q, Zhu X, He Y, Yang W. Partial oxidation of methane in $BaCe_{0.1}Co_{0.4}Fe_{0.5}O_{3\text{-delta}}$ membrane reactor. *Catal Today*. 2010;149: 185–190.
52. Gu XH, Jin WQ, Chen CL, Xu NP, Shi J, Ma YH. YSZ-$SrCo_{0.4}Fe_{0.6}O_{3\text{-delta}}$ membranes for the partial oxidation of methane to syngas. *AIChE J*. 2002;48:2051–2060.

Manuscript received Feb. 6, 2015, and revision received Apr. 3, 2015.